Macromolecules

pubs.acs.org/Macromolecules Article

# User Guide to Ring-Opening Metathesis Polymerization of *endo*-Norbornene Monomers with Chelated Initiators

Henry L. Cater, Iana Balynska, Marshall J. Allen, Benny D. Freeman, and Zachariah A. Page*

Cite This: *Macromolecules* 2022, 55, 6671−6679 Read Online

ACCESS | Metrics & More | Article Recommendations | Supporting Information

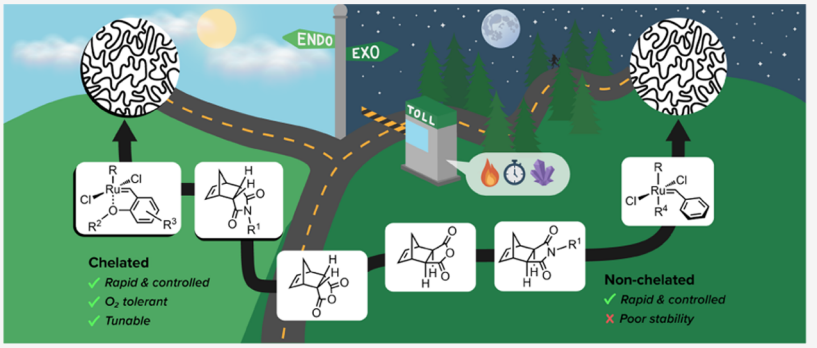


**ABSTRACT:** The development of facile synthetic strategies to access well-defined polymers promises to provide advanced soft materials with functionality that rivals that observed from nature. To this end, ring-opening metathesis polymerization (ROMP) presents a compositionally simple and rapid strategy for controlled polymerization, yet it has received far less attention relative to radical counterparts. This limited attention arises in part from scattered reports on optimization strategies and a narrow monomer scope. Contemporary ROMP methods favor the use of *exo*-norbornene derivatives and highly reactive nonchelated Ru-alkylidenes, such as Grubbs Catalysts. In contrast, *endo*-norbornene derivatives, from which analogous *exo*-forms are often generated, present a more accessible alternative, yet examples of their utility in ROMP remain scarce. Herein, a systematic examination of ROMP with *endo*-norbornene monomers using stable chelated Ru-alkylidene initiators is presented. Through initiator screening and polymerization optimization, the ROMP process is shown to be versatile and robust, providing rapid access to polymers with excellent molecular weight control, low dispersities ($Đ$ < 1.1), good functional group tolerance, and high chain-end fidelity that enabled the preparation of block copolymers via sequential monomer addition. Furthermore, the process is oxygen-tolerant, allowing for ROMP to be performed under ambient conditions on the bench, which was showcased in synthesizing mechanically robust *endo*-norbornene imide thermoplastics with high glass transition and decomposition temperatures. This report provides a comprehensive overview of the scope and limitations of *endo*-norbornene ROMP with chelated initiators, serving as a user guide for the polymer chemistry community to develop well-defined next-generation functional plastics.



## INTRODUCTION

The sophistication and associated functionality of current synthetic materials pale in comparison to those found in nature due to limitations in controlled polymerization methodologies.[1−3] These limitations include a lack of rapid and economical strategies to control composition, architecture, and size. Contemporary controlled polymerization strategies include those that proceed via ionic, radical, or metathetic mechanisms.[4] Among these, ring-opening metathesis polymerization (ROMP) offers an unrivaled combination of speed, control, functional group tolerance, and simplicity (fewer reagents and milder reaction conditions).[5] Despite its merits, the ROMP of strained cyclic olefins has received much less attention relative to controlled radical polymerizations of acrylics via atom transfer radical polymerization and radical addition fragmentation chain transfer. Primary obstacles to widespread implementation of ROMP are high cost,[6] limited monomer accessibility, and the requirement for air-free reaction conditions.[7]

Inexpensive, industrially relevant cyclic olefin monomers are commercially available (e.g., $31/kg for norbornene and $66/kg for cyclooctene),[8,9] but functionalized derivatives are rare and expensive (e.g., >$65/g for *exo*-5-norbornenecarboxylic acid).[10] Although *exo*-5-norbornenecarboxylic acid is one of the most commonly employed functional monomer precursors

Received: June 8, 2022
Revised: July 12, 2022
Published: July 26, 2022

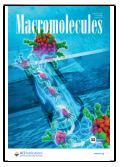





https://doi.org/10.1021/acs.macromol.2c01196
*Macromolecules* 2022, 55, 6671−6679

for ROMP, 5-norbornene-*endo*-2,3-dicarboxylic anhydride represents an attractive low-cost alternative (e.g., <$15/kg)[11,12] that can be easily transformed into a diverse array of functional diester or imide monomers in a single step. However, literature examples conventionally use *exo*-norbornene monomers[13−26] for ROMP owing to their reduced steric encumbrance and concomitantly increased reactivity and polymerization control relative to their endo-counterparts.[27−30] Although reports on ROMP of *endo*-norbornene monomers exist,[31−34] the utility of stable chelated initiators in combination with these less reactive, yet more accessible *endo*-derivatives has not been systematically examined. The reduced accessibility of *exo*-norbornene imide monomers arises in part from the requisite *endo*-to-*exo* isomerization for norbornene-anhydride that is both energy (~180 to 250 °C) and time/material intensive (up to 16 h reaction time and as many as six recrystallizations from benzene with <20% overall yield).[14,35−37] From an applied perspective, *endo*-norbornene imide polymers have been observed to possess higher glass transition temperatures relative to their *exo*-analogues, a likely consequence of increased segmental packing and energetic barriers to backbone rotation while retaining comparable thermal stability and mechanical performance.[32,38] Thus, a rapid and controlled polymerization strategy for *endo*-norbornene monomers using a tunable and stable metathesis initiator would be of significant utility to the polymer science community.

Exacerbating the hurdles to widespread implementation of ROMP are the oxygen sensitivity (particularly in solution)[39] and high cost (~$70 to $500/g)[40,41] of widely adopted ruthenium alkylidene initiators. To address stability issues, Hoveyda and co-workers developed ruthenium initiators that possess an internal oxygen chelate, which has enabled purification by chromatography.[42,43] While these complexes have greatly improved air and moisture stability relative to analogous Grubbs Catalysts, they have primarily been utilized for ring-closing metathesis and cross-metathesis, with only a few reports of ROMP in the literature.[44−47] To the issue of cost, recent work on catalytic ROMP via degenerative chain transfer by Kilbinger and co-workers[48−50] and metal-free ROMP by Boydston and co-workers[51,52] paves an avenue toward more economical strategies while maintaining a controlled polymerization.

Herein, the rapid and controlled polymerization of *endo* feedstock monomers using bench-stable chelated ruthenium initiators is systematically examined (Figure 1). The key to polymerization control is the reduced propagation rates of *endo*-monomers (relative to *exo*) complemented by the reduced initiation rates of chelated initiators. Despite these reduced rates, quantitative monomer-to-polymer conversion is possible in under 2 h. To this effect, a small library of chelated ruthenium initiators with varying stereoelectronic properties was examined and compared for their ROMP of *endo*-norbornene monomers. The addition of triphenylphosphine ($PPh_3$) provided polyolefins with narrow-molecular-weight distributions ($Đ$ < 1.1) and enabled the one-pot preparation of block copolymers. Moreover, the employment of *endo*-norbornene monomers enabled the use of chelated initiators for controlled ROMP under ambient conditions, which provided facile access to mechanically robust thermoplastics bearing high glass transition and decomposition temperatures. The present manuscript showcases a user-friendly approach to perform ROMP that is anticipated to both motivate and inform further monomer and initiator development to harness more sophisticated, next-generation functional plastics.

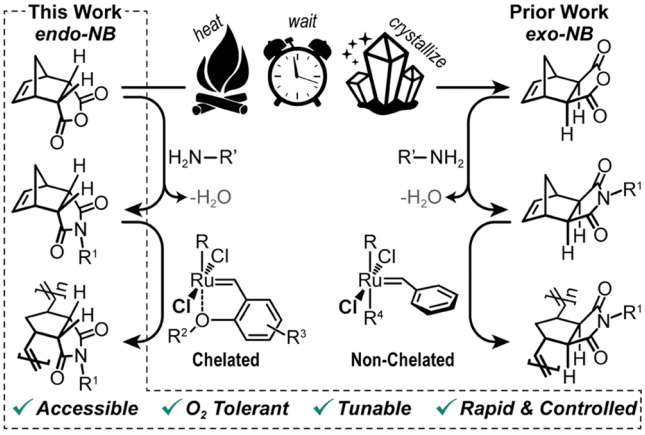


**Figure 1.** Overview of the contemporary preparation and use of *exo*-norbornene monomers in ring-opening metathesis polymerization (ROMP) with nonchelated ruthenium alkylidenes (right) in juxtaposition with the current work on ROMP of *endo*-norbornene monomers with more stable chelated ruthenium alkylidenes (left).

## RESULTS AND DISCUSSION

**Initiator Screening.** Butyl norbornene imide (NBI) was selected as the prototypical *endo*-monomer for initial studies due to the corresponding polymer's anticipated solubility in organic solvents granted by the aliphatic side chain. The facile synthesis of these *exo*- and *endo*-NBI monomers was carried out by refluxing *exo*- or *endo*-*cis*-5-norbornene-2,3-dicarboxylic anhydride in toluene with 1.2 equiv of readily available 1-butylamine in the presence of catalytic triethylamine. Purification involved solvent removal followed by flash silica gel chromatography with ethyl acetate as the eluent, providing the two isomers in a good isolated yield (>80%). To examine ROMP of NBI monomers (Figure 2a), a selected few of the most prevalent and commercially available ruthenium alkylidene initiators were screened (Figure 2b). Namely, Grubbs Catalyst 1st (**G1**), 2nd (**G2**), and modified 3rd (**G3′**)—in which pyridine ligands replace 3-bromopyridine used for **G3**—generations along with Hoveyda−Grubbs Catalyst 1st (**HG1**) and 2nd (**HG2**) generations were tested.

Initial polymerizations to compare Ru-based initiators were carried out inside of a nitrogen-filled glovebox at room temperature (Figure 2). A starting monomer concentration ($[M]_0$) of 0.5 M was used, along with a target degree of polymerization (DP) of 250 to showcase a rapid route to high-molecular-weight polymers ($M_{n(theory)}$ = 55 kg/mol). Reactions were tracked using $^1$H NMR to determine monomer-to-polymer conversion. Gel permeation chromatography (GPC) was employed to estimate molecular weight and dispersity ($Đ$) (relative to polystyrene standards). For *endo*-NBI, it was observed that **HG2** and **G3′** resulted in full monomer conversion ~2× faster than observed using **G2** in a variety of solvents (Table S1 in the Supporting Information). Little-to-no conversion was observed using **G1** and **HG1** within 15 min. Narrow-molecular-weight distributions were achieved with **HG2** and **G3′** ($Đ$ < 1.3), with the smallest dispersities obtained when employing tetrahydrofuran (THF) as the solvent ($Đ$ < 1.2). In contrast to the ROMP of *endo*-NBI with **HG2**, ROMP of *exo*-NBI under equivalent conditions resulted in large dispersities ($Đ$ > 2.6) (Figure 2c). Alternatively, **G3′**


https://doi.org/10.1021/acs.macromol.2c01196
Macromolecules 2022, 55, 6671−6679

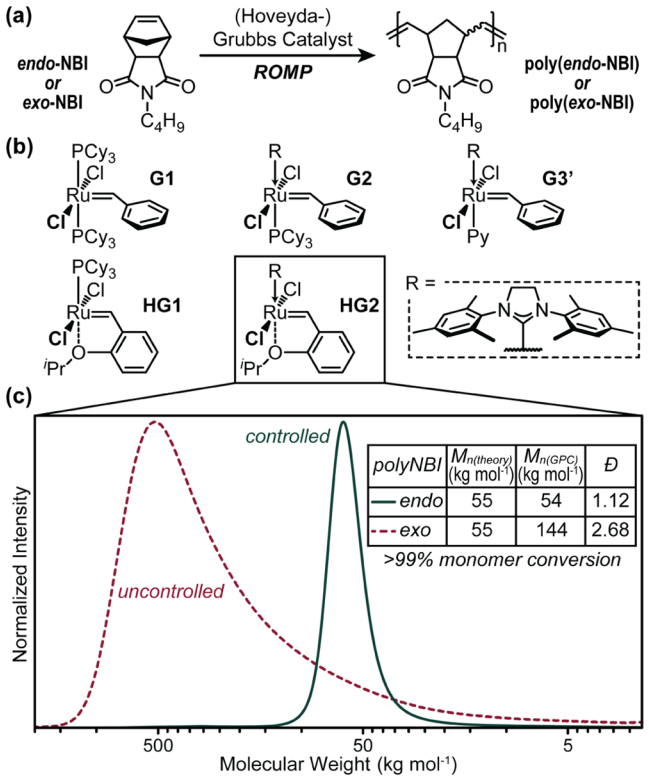


**Figure 2.** ROMP of *endo*- and *exo*-norbornene imide (NBI) derivatives. (a) Polymerization schematic. (b) Chemical scope of initial ruthenium alkylidenes examined. (c) Overlaid gel permeation chromatograms of poly(*endo*-NBI) and poly(*exo*-NBI) prepared with Hoveyda−Grubbs Catalyst 2nd generation (**HG2**).

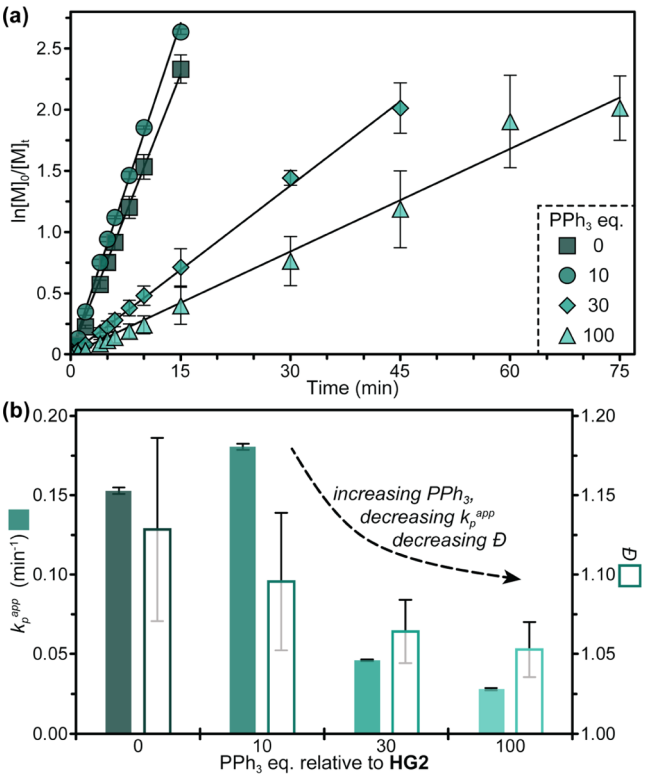


**Figure 3.** Effect of $PPh_3$ loading on polymerization kinetics and molecular weight distributions for *endo*-NBI with **HG2**. (a) Plot of the natural log change in molecular weight over time with linear fit (black line). (b) Bar chart of the apparent polymerization rate ($k_p^{app}$) and dispersity ($Đ$). Error bars represent ± one standard deviation from the mean.

maintained good control over polymerization of *exo*-NBI ($Đ$ < 1.05). The distinction in polymerization control is attributed to a combination of faster propagation for *exo*-NBI relative to *endo*-NBI[27−30] and slower initiation for the chelated **HG2** initiator relative to **G3′**.[53,54] For further ROMP studies with *endo*-monomers, **HG2** was selected as the initiator of choice due to its purported superior bench and solution stability relative to traditionally employed **G3′**,[55,56] in addition to its similarly rapid polymerization rate.

**Polymerization Optimization.** In an effort to improve control over *endo*-NBI ROMP using **HG2**, ligands were incorporated into the reaction mixture to reduce the rate of propagation such that all chains initiate and grow simultaneously. Specific ligands examined were triphenylphosphine ($PPh_3$) and 3-bromopyridine (3-BrPy), which are both capable of reversibly binding ruthenium alkylidene initiators (Tables S4−S10 in the Supporting Information). Thus, these ligands act as antagonists (competitors) with respect to alkene binding, improving control over ROMP. In combination with *endo*-NBI and **HG2**, both $PPh_3$ and 3-BrPy were found to effectively reduce $Đ$. Further experimentation was performed using $PPh_3$ due to its reduced toxicity, cost, and ease of handling relative to 3-BrPy. Optimization of $PPh_3$ loading was performed by monitoring the ROMP of *endo*-NBI with **HG2** (Figure 3). $^1$H NMR revealed a linear correlation between the natural log change in monomer concentration over time ($\ln[M]_0/[M]_t$), which is indicative of a controlled polymerization[57] (Figure 3a). From this result, the apparent rate constant of propagation ($k_p^{app}$) was determined from the slope.[57] This showed that as $PPh_3$ loading was increased, $k_p^{app}$ generally decreased: 0.153 ± 0.002, 0.181 ± 0.002, 0.046 ± 0.001, and 0.028 ± 0.001 $min^{-1}$ for 0, 10, 30, and 100 equiv of $PPh_3$ relative to **HG2**, respectively (Figure 3b). It is hypothesized that the modest increase in $k_p^{app}$ at small $PPh_3$ loadings (10 equiv relative to **HG2**) results from a fast equilibration between $PPh_3$ and **HG2** leading to the formation of a more rapidly initiating phosphine-coordinated initiator in situ, prior to the first monomer addition.[58] This rapidly initiating species serves to increase the overall apparent rate more so than the antagonistic effect of $PPh_3$ on slowing propagation. GPC analysis showed a trend toward decreased $Đ$ upon increasing $PPh_3$ loading: 1.13 ± 0.06, 1.10 ± 0.02, 1.06 ± 0.02, and 1.05 ± 0.02 for 0, 10, 30, and 100 equiv of $PPh_3$ (Figure 3b). Given the trade-off between $k_p^{app}$ and $Đ$ upon increasing $PPh_3$, further studies compromised by primarily using 30 equiv of $PPh_3$ relative to **HG2**.

**Platform Scope.** Initial versatility assessment surrounded the effect of the monomer-to-**HG2** ratio on polymerization control (Table 1, entries 1−5). To identify upper limitations, 30 equiv of $PPh_3$ relative to **HG2** were used in variable DP studies. ROMP of *endo*-NBI at a target DP = 500 was complete within 4 h, and GPC revealed molecular weight values near theoretical and low $Đ$ (Table 1, entry 1). The first attempts to target a DP of 1000 were accomplished at a reduced monomer concentration (0.1 M) to avoid issues associated with high reaction viscosity. However, despite high monomer conversion (98%), under dilute conditions, deleterious side reactions dominated, such as "back-biting" and/or cross-metathesis,[59] which led to a loss of polymerization control. To favor polymer


https://doi.org/10.1021/acs.macromol.2c01196
Macromolecules 2022, 55, 6671−6679

**Table 1. ROMP Versatility of *endo*-Norbornene Monomers with HG2**

| entry | monomer | equiv $PPh_3$ | [monomer] (M) | NBI comonomer (5 mol %) | target DP | time (h) | conv.$_{(NMR)}$ (%) | $M_{n,GPC}$ ($M_{n,theo}$) (kg/mol) | $Đ$ |
|---|---|---|---|---|---|---|---|---|---|
| **1** | *endo*-NBI | 30 | 0.5 | | 500 | 4.0 | >99 | 111 (110) | 1.14 |
| **2** | | | 0.1 | | 1000 | 16.0 | 98 | 26 (219) | 1.57 |
| **3** | | | 1.0 | | 1000 | 2.0 | 97 | 214 (219) | 1.17 |
| **4** | | | 1.0 | | 1500 | 2.0 | 91 | 273 (329) | 1.34 |
| **5** | | | 1.0 | | 2000 | 2.0 | 76 | 377 (439) | 1.43 |
| **6** | *endo*-NBI | 30 | 0.5 | −OH | 250 | 4.0 | >99 | 54 (55) | 1.11 |
| **7** | | | | −SMe | | | >99 | 56 (55) | 1.11 |
| **8** | | | | $-NH_2$ | | | 7 | 6 (55) | 1.21 |
| **9** | | | | −COOH | | | >99 | 57 (56) | 1.17 |
| **10** | | | | $-NMe_2$ | | | >99 | N/A[a] (55) | N/A[a] |
| **11** | *endo*-NBdE | 0 | 0.5 | | 250 | 0.5 | >99 | 75 (74) | 1.20 |
| **12** | | 10 | | | | 1.0 | >99 | 81 (74) | 1.08 |
| **13** | | 30 | | | | 1.5 | 99 | 81 (74) | 1.05 |
| **14** | | 100 | | | | 2.0 | 89 | 74 (74) | 1.04 |

[a]GPC data not obtained for entry **10** due to presumed column interactions precluding sample elution.

chain growth over metathetic side reactions, ROMP was performed at an increased monomer concentration (1.0 M). For example, targeting a DP of 1000 at a monomer concentration of 0.1 vs 1.0 M provided a $Đ$ of 1.57 vs 1.17, respectively (Table 1, entries 2 and 3). At these higher concentrations, poly(*endo*-NBI) with molecular weights in excess of 375 kg/mol (DP ≈ 1700) was achievable; however, the $Đ$ values notably increased to 1.34 and 1.43 when targeting a DP of 1500 and 2000, respectively (Table 1, entries 3−5). Moreover, the relative number average molecular weight from GPC ($M_{n,GPC}$) began to deviate to a greater extent at target DPs beyond 1000, which represents a potential chain-length maximum for the current conditions.

To further assess versatility of the present platform, a small series of functionalized *endo*-monomers were synthesized and evaluated as comonomers with *endo*-NBI (Figure 4 and Table 1, entries 6−10). Specifically, primary alcohol, thioether, primary amine, carboxylic acid, and tertiary amine functionality were examined. For clarity, the corresponding naming system of functional monomers was used: *endo*-NBI−X where X is −OH, −SMe, $-NH_2$, −COOH, or $-NMe_2$. To mitigate issues with polymer solubility in THF, which is used as the reaction solvent as well as for GPC analysis, each functional group was incorporated as 5 mol % of the overall monomer feed alongside *endo*-NBI, at a target DP = 250. Each polymerization was run for 4 h, at which point $^1$H NMR spectroscopy revealed complete conversion (and thus incorporation) of all functional group monomers with the exception of *endo*-NBI−$NH_2$ (7% conversion). It is hypothesized that the nucleophilic primary amine poisoned **HG2**, precluding ROMP, as previously observed for other Grubbs Catalysts.[60] ROMP with *endo*-NBI−OH, −SMe, and −COOH monomers maintained good control, as indicated by low dispersities ($Đ$ < 1.2). Attempts to characterize polymers containing $-NMe_2$ functionality by GPC proved unsuccessful, which is attributed to the basicity of the amine resulting in column interactions. Overall, the demonstrated functional group tolerance provides a useful handle to facilitate polymer post-modification processes and/or polymer self-assembly.

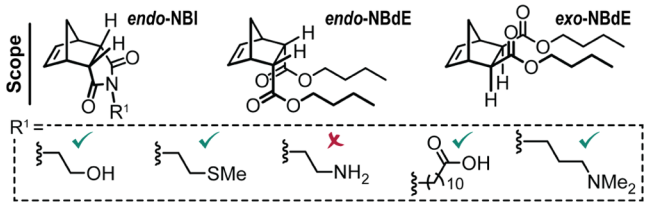


**Figure 4.** Chemical structures for norbornene monomers examined using **HG2** for ROMP. The check marks represent functional group tolerance using the present approach. The primary amine derivative, *endo*-NBI−$NH_2$, was the only one that prevented ROMP under the current conditions.

As a final measure of versatility, an additional class of inexpensive and synthetically accessible *endo*-norbornene monomers was examined using the present **HG2** ROMP conditions. Specifically, *endo*-norbornene butyldiester (*endo*-NBdE) was synthesized in a high yield (>80%) from the same starting material as *endo*-NBI, namely, *cis*-5-norbornene-*endo*-2,3-dicarboxylic anhydride. The aforementioned starting material was heated to 75 °C with an excess of 1-butanol in the presence of an acid catalyst for 16 h, followed by removal of butanol under reduced pressure, acid neutralization, and drying to give the product. Relative to *endo*-NBI, ROMP of *endo*-NBdE with **HG2** was found to be ∼1.25× faster ($k_p^{app}$ = 0.191 ± 0.007 $min^{-1}$ without $PPh_3$) (Table S13 in the Supporting Information). The enhanced polymerization rate is postulated to arise from reduced Ru-chelation strength of *endo*-NBdE relative to *endo*-NBI.[27] In the absence of $PPh_3$, $Đ$ values ≤1.2 were obtained (Table 1, entry 11). Addition of $PPh_3$ again resulted in significant improvements in $Đ$, with values <1.1 (Table 1, entries 12−14). For completeness, the analogous *exo*-norbornene butyldiester (*exo*-NBdE) was synthesized and polymerized with **HG2**, showing reduced control over molecular weight and dispersity ($Đ$ > 1.35) (Table S3 in the Supporting Information).

An attractive feature of oxygen-chelated ruthenium alkylidenes is their design scope with regard to stereoelectronic tunability.[61−64] In this respect, three additional oxygen-chelated initiators bearing different functionalities designed to facilitate rapid initiation were examined (Figure 5). All initiators were analogous to **HG2** but respectively contained the following groups relative to the Ru alkylidene: 2-methoxy chelate (**methoxy-HG2**),[65] 5-nitro substituent (discovered by Grela and co-workers) (**nitro-Grela**),[66] and a 3-phenyl substituent discovered by Blechert and co-workers (**Ble-**


https://doi.org/10.1021/acs.macromol.2c01196
Macromolecules 2022, 55, 6671−6679

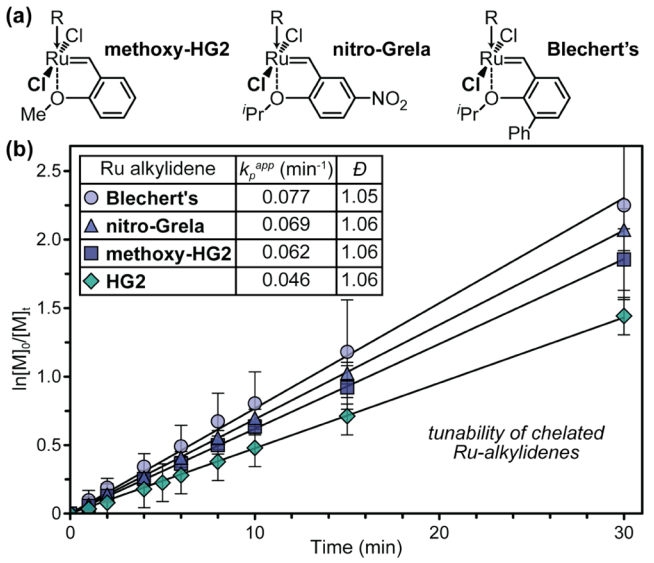


**Figure 5.** ROMP of *endo*-NBI as a function of the oxygen-chelated ruthenium alkylidene initiator employed. (a) Chemical structures for the three additional derivatives examined. (b) Plot of the natural log change in molecular weight over time with linear fit (black line) and inset tabulating the resultant $k_p^{app}$ and Đ.

chert's)[67] (Figure 5a). Using 30 equiv of $PPh_3$ relative to each Ru-alkylidene, ROMP was found to result in comparably low Đ (<1.1) and faster $k_p^{app}$ relative to **HG2** (Figure 5b). The most rapid ROMP occurred when employing **Blechert's** catalyst, providing a $k_p^{app}$ of 0.077 ± 0.001 min$^{-1}$, ~1.7× faster than **HG2**, which is attributed to its faster rate of initiation.[45,68]

**Block Copolymers.** To assess the "livingness" of the present platform, chain-end fidelity was examined through sequential *endo*-NBI monomer addition to form pseudo-block copolymers. Targeting a DP = 100, poly(*endo*-NBI) was synthesized with **HG2** in the presence of 30 equiv $PPh_3$. At 90 min intervals, *endo*-NBI was added (DP = 100 for each block), immediately prior to which a small aliquot was removed for GPC and $^1$H NMR analysis, with the latter confirming near-quantitative monomer conversion at each block (Table S17 in the Supporting Information). This process was repeated to successfully yield a pseudo-hexablock polymer (DP ≈ 600) with Đ < 1.2. This demonstrated a high degree of controlled chain growth up to as many as five extensions (Figure 6a). Additionally, a mixed ABA triblock copolymer (Đ = 1.13) and an ABABA pentablock copolymer (Đ = 1.22) were successfully synthesized from alternating DP = 100 poly(*endo*-NBI) and poly(*endo*-NBdE) homopolymer subunits (Figure S12 and Table S18 in the Supporting Information). It is postulated that marginally increased Đ with the block copolymer systems resulted from (1) ruthenium chain-end decomposition at longer reaction times and/or (2) reduced steric hindrance surrounding the NBdE repeat units in the mixed block copolymer case, leading to increased cross-metathesis.

Modest increases in Đ with each block addition prompted an investigation into quantifying the chain-end fidelity of the present ROMP method. This was accomplished by preparing pseudo-diblock copolymers and examining the effects of prolonged time delays in monomer addition between the first and second blocks after the first block had reached full monomer conversion (Figures 6b and S13 and Table S19 in the Supporting Information). It was qualitatively observed that

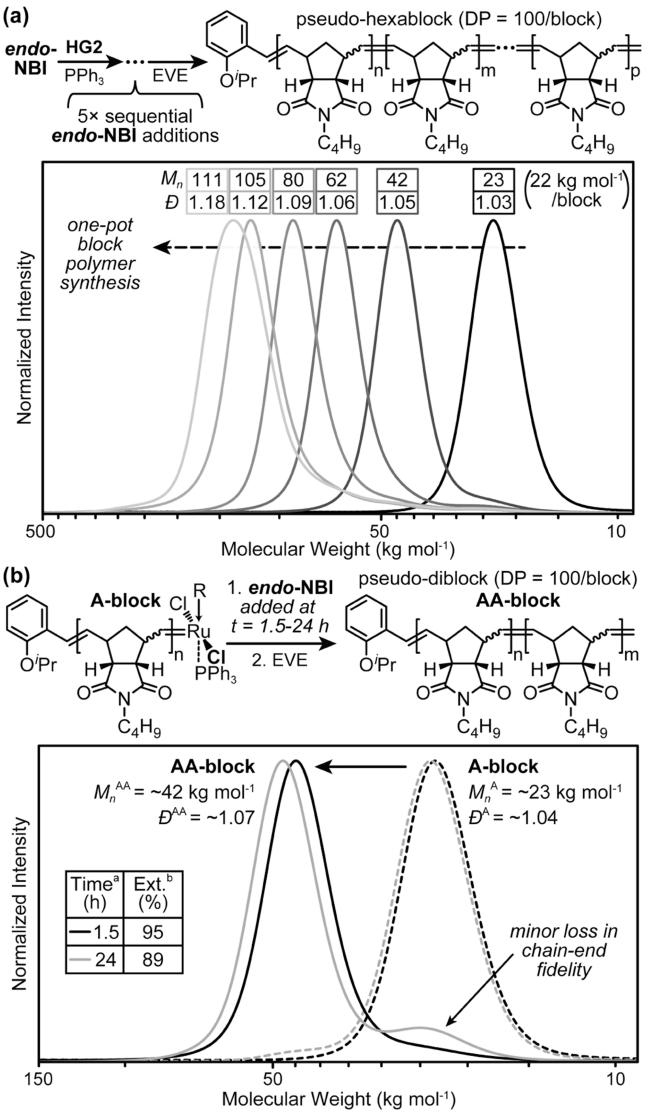


**Figure 6.** Poly(*endo*-NBI) chain extensions. (a) Polymerization schematic for pseudo-hexablock synthesis with GPC plots of molecular weight vs normalized signal intensity for each block. (b) Overlaid GPC traces for A-block and AA-diblock polymers, where the second monomer addition was performed at different times after ~quantitative monomer consumption to form the first A-block to demonstrate good chain-fidelity. [a]Polymerization time for the first A-block, corresponding to the point of second monomer addition. [b]Percent chain extension (Ext.) was calculated by integrating two Gaussians of best fit, described in the Supporting Information.

GPC traces of the AA-diblocks had increasingly larger residual A-block (homopolymer) signals for longer delay times prior to the second monomer addition. This lack of chain extension was attributed to a loss in chain-end activity (i.e., a decrease in chain-end fidelity) that likely arises from side reactions, such as back-biting or cross-metathesis. In an effort to quantify the chain-end fidelity, GPC trace deconvolution was accomplished by fitting each curve with two Gaussian distributions and taking the relative area under each as a representation of the AA-diblock to A-block ratio (further details are provided in the Supporting Information). Note that this process assumes that there is no significant change in the refractive index upon chain extension. From this fitting process, it was found that 95% of chains extended if the monomer was added at 1.5 h, which


https://doi.org/10.1021/acs.macromol.2c01196
Macromolecules 2022, 55, 6671−6679

decreased to 89% if the reaction was allowed to stir for 24 h prior to monomer addition. This roughly corresponds to a 0.3% loss in chain-end fidelity per hour using the present ROMP process of *endo*-NBI (Figure S15 in the Supporting Information). Notably, performing the same analysis on *exo*-NBI revealed a 3.4% loss in chain-end fidelity per hour (Figure S16 and Table S21 in the Supporting Information). The improved stability in chain-end fidelity observed for poly(*endo*-NBI) relative to poly(*exo*-NBI) is hypothesized to arise from greater steric interactions that reduce metathetic side reactions, making *endo*-NBI monomers better suited for the one-pot preparation of block copolymers.

**Bench Polymerizations.** As a testament to the superior solution stability and utility of chelated initiators, such as **HG2**, relative to the traditionally employed **G3′** initiator, stock solutions (0.025 M in THF) of both were independently prepared on the bench under ambient conditions and used to synthesize poly(*endo*-NBI) (target DP = 250) in capped vials under an air atmosphere (~77% headspace). To date, the use of chelated initiators in air has been limited to ring-closing metathesis reactions, where, unlike ROMP, large catalyst loadings can be implemented, and side reactions do not mitigate product formation.[69] In our method, polymerizations were set up at 2 h intervals following initiator stock solution preparation and allowed to progress for 90 min before quenching with excess ethyl vinyl ether. Resultant poly(*endo*-NBI) samples were characterized using GPC and $^1$H NMR spectroscopy (Figure 7). ROMP with **HG2** and 30 equiv of $PPh_3$ provided polymers with $Đ$ < 1.2 up to and including 8 h following initiator solution preparation. Notably, monomer conversion at 90 min decreased slightly as the initiator stock solution aged, from 95 to 82% conversion when using 0 and 8 h stocks, respectively. This suggests that the initiator activity decreased when stored under ambient conditions in solution. In contrast, poly(*endo*-NBI) prepared using **G3′** stock solutions (with and without $PPh_3$, see Table S22 in the Supporting Information) had significantly reduced control, as indicated by lower monomer conversions for samples prepared using >2 h old initiator stocks, polymer molecular weights exceeding targets in all cases (55 kg/mol), and increasing $Đ$ upon stock aging (>2.0 when using >4 h old initiator stocks).

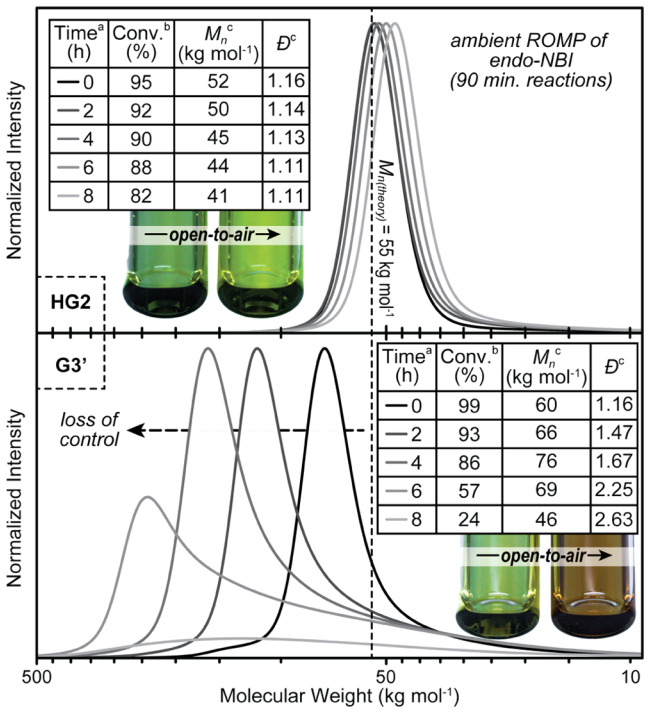


**Figure 7.** GPC traces for poly(*endo*-NBI) samples prepared via ambient ROMP on the bench using **HG2**- (top) and **G3′**- (bottom) stock solutions. Polymerizations were initiated at varying times after initiator stock solution preparation ($t$ = 0). Insets—images of the bottom half of vials laying down that contain initiator stock solutions before and after air exposure, showing a visible color change for **G3′** solutions. [a]Time from initiator stock preparation. [b]Conversion determined by $^1$H NMR. [c]$M_n$ and $Đ$ determined by GPC.

The difference in control was attributed to an increased oxygen stability for **HG2** relative to **G3′**, which was qualitatively indicated by a color change from green to brown for the **G3′** stock solutions and little color change for the **HG2** solutions (Figure 7, inset). Additionally, ambient polymerization using a **G2** initiator stock solution prepared in air, with 30 equiv of $PPh_3$, resulted in a significant loss of control (e.g., low monomer conversion and increasing $Đ$ to ~1.7 over an 8 h initiator stock lifetime) (Figure S17 and Table S23 in the Supporting Information). Degradation was corroborated by comparative $^1$H NMR studies of **HG2** and **G3′** in solution, prepared under both ambient and inert conditions. The percentage of the active initiator was quantified by monitoring the alkylidene signals over time at ~16.5 and ~19.2 ppm for **HG2** and **G3′**, respectively, relative to an internal standard (anthracene). This revealed a little-to-no decrease in the signal for **HG2** relative to **G3′**, along with an accelerated degradation for G3′ solutions prepared under ambient conditions (Figure S18 in the Supporting Information).

To showcase the utility of air-tolerant ROMP in accessing thermomechanically robust materials, poly(*endo*-NBI) prepared on the benchtop and poly(*exo*-NBI) prepared under inert conditions were compared using a suite of standard characterization methods (Figures 8 and S3−S7 in the Supporting Information). For consistency, molecular weights were all ~100 kg/mol. Moreover, hydrogenation was performed to expand the material scope and compare the unsaturated polymers to their more oxidatively stable saturated analogues.[70] Thermogravimetric analysis revealed similarly high 5% mass thermal decomposition temperatures ($T_{d5}$) of 380 and 400 °C for the *endo*- and *exo*-NBI polymers, respectively (Figure 8a). Differential scanning calorimetry (both standard and modulated) revealed glass transition temperature ($T_g$) values nearly 50 °C higher for the unsaturated *endo*- relative to *exo*-NBI polymers (169 ± 5 and 120 ± 3 °C, respectively, Figure 8b). Upon hydrogenation, $T_g$ values decreased, yet the *endo*-NBI derivatives were still ~30 °C higher relative to their *exo*-NBI counterparts (118 ± 3 and 87 ± 2 °C, respectively). These results are in-line with prior reports and hypothesized to arise from improved packing of the *endo*-NBI polymers.[32] Finally, tensile testing on dogbone specimens punched from sheets of the four thermoplastics was accomplished to characterize the mechanical performance (Figure 8c). In doing so, all materials were found to be strong rigid plastics, with max stress ($\sigma_m$) ranging from 32 to 40 MPa and moduli ($E$) from 1.3 to 1.9 GPa. In general, hydrogenation produced stronger and stiffer polymers relative to the unsaturated precursors. Overall, it was shown that poly(*endo*-NBI) materials prepared under ambient conditions represent promising candidates for applications that require high $T_g$,


https://doi.org/10.1021/acs.macromol.2c01196
Macromolecules 2022, 55, 6671−6679

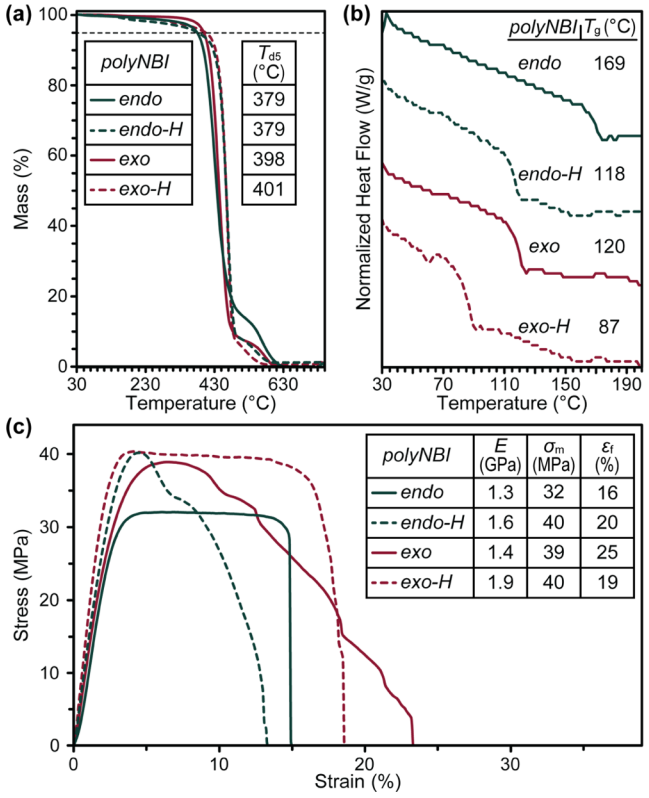


**Figure 8.** Thermomechanical characterization of poly(*endo*-NBI) prepared by ROMP under ambient conditions and poly(*exo*-NBI) prepared under inert conditions, along with their corresponding hydrogenated derivatives. (a) Thermogravimetric analysis. (b) Differential scanning calorimetry with traces stacked for clarity. (c) Stress−strain data from uniaxial tensile testing. $T_{d5}$ = thermal decomposition temperature at 5% mass loss; $T_g$ = glass transition temperature; $E$ = Young's modulus (stiffness); $\sigma_m$ = max stress (strength); and $\varepsilon_f$ = strain at failure.

thermal stability, and mechanically strong and rigid thermoplastics.

## CONCLUDING REMARKS

A rapid, controlled, and accessible approach to ROMP that makes use of readily available *endo*-monomers and solution-stable chelated initiators was showcased. A diverse array of functionalized monomers were synthesized in a single step from inexpensive starting materials and optimal conditions for their controlled polymerizations up to 375 kg/mol were identified. The use of triphenylphosphine as an additive enabled the preparation of uniform polymer chains with $Đ$ < 1.1, reaching ~quantitative monomer conversion in 90 min or less. The versatility of the conditions presented was demonstrated by the incorporation of carboxylic acid, thioether, alcohol, and tertiary amine functionality into polymer backbones. The effect of altering the initiator alkylidene groups on the rate of polymerization was evaluated by examining methoxy-HG2, Blechert's, and nitro-Grela initiators. In doing so, it was revealed that subtle stereoelectronic variations affect the overall rate of polymerization, demonstrating the tunability of chelated initiators. Block copolymer syntheses were successfully carried out, showing only marginal losses in chain-end fidelity over long periods of time. Furthermore, highly controlled benchtop polymerizations were demonstrated under ambient conditions using **HG2**, in contrast to the rapid loss of control observed when employing the more traditional **G3′** ROMP initiator. Finally, ROMP of *endo*-NBI under ambient conditions provided thermoplastics with $T_g$ values higher than their *exo*-NBI counterparts while maintaining good thermal stability, mechanical strength, and rigidity. Thus, the present systematic report on an *endo*/chelated initiator ROMP platform serves to broaden the scope of tools at one's disposal when designing sophisticated soft materials such as block copolymers, thermoplastics, or thermoplastic elastomers. It is envisioned that this work will both encourage and inform the use of ROMP as a viable approach that, together with other emergent strategies, will pave the way toward accessible next-generation plastics.

## ASSOCIATED CONTENT

### Supporting Information

The Supporting Information is available free of charge at https://pubs.acs.org/doi/10.1021/acs.macromol.2c01196.

Materials, experimental and instrumentation details, including synthetic methods, polymerization procedures, kinetics data, initiator degradation studies, thermal characterization (TGA and DSC), MATLAB coding, chain-end fidelity studies, and $^{1}H$ and $^{13}C$ NMR data (PDF)

## AUTHOR INFORMATION

### Corresponding Author

**Zachariah A. Page** − *Department of Chemistry, The University of Texas at Austin, Austin, Texas 78712, United States;* orcid.org/0000-0002-1013-5422; Email: zpage@utexas.edu

### Authors

**Henry L. Cater** − *Department of Chemistry, The University of Texas at Austin, Austin, Texas 78712, United States*

**Iana Balynska** − *Department of Chemistry, The University of Texas at Austin, Austin, Texas 78712, United States*

**Marshall J. Allen** − *McKetta Department of Chemical Engineering, The University of Texas at Austin, Austin, Texas 78712, United States*

**Benny D. Freeman** − *McKetta Department of Chemical Engineering, The University of Texas at Austin, Austin, Texas 78712, United States;* orcid.org/0000-0003-2779-7788

Complete contact information is available at: https://pubs.acs.org/10.1021/acs.macromol.2c01196

### Author Contributions

The manuscript was written through contributions of all authors. All authors have given approval to the final version of the manuscript. H.L.C. and Z.A.P. were responsible for conceptualization and visualization, H.L.C., I.B., and M.J.A. for data curation, formal analysis, investigation, methodology, and validation, and Z.A.P. and B.D.F. for project administration, resources, and supervision.

### Notes

The authors declare no competing financial interest.

## ACKNOWLEDGMENTS

This material is based upon work supported by the National Science Foundation under Grant No. DMR-2045336 (H.L.C., I.B., and Z.A.P., synthesis and kinetics, composition, and molecular weight characterization). This work was supported

as part of the Center for Materials for Water and Energy Systems (M-WET), an Energy Frontier Research Center funded by the U.S. Department of Energy, Office of Science, Basic Energy Sciences under Award #DE-SC0019272 (M.J.A. and B.D.F., thermal characterization). This material is based upon work supported by the National Science Foundation Graduate Research Fellowship under Grant No. DGE-1610403 (M.J.A.). For partial financial support, the authors thank the Robert A. Welch Foundation under Grant No. F-2007 (Z.A.P.) and Grant No. F-1924-20170325 (B.D.F.). The authors acknowledge the use of shared research facilities supported in part by the Texas Materials Institute. The authors would also like to thank Umicore for supplying C599 (methoxy-HG2 catalyst) and C703 (Blechert's catalyst) and Mado Hayes for assistance with the Table of Content graphic.

## ■ ABBREVIATIONS

ROMP, ring-opening metathesis polymerization; *Đ*, dispersity; G1, Grubbs Catalyst 1st generation; G2, Grubbs Catalyst 2nd generation; G3′, modified Grubbs Catalyst 3rd generation; HG1, Hoveyda−Grubbs Catalyst 1st generation; HG2, Hoveyda−Grubbs Catalyst 2nd generation; *DP*, degree of polymerization; THF, tetrahydrofuran; NBI, norborneneimide; NBdE, norbornene butyldiester

## ■ REFERENCES

(1) Wegst, U. G. K.; Bai, H.; Saiz, E.; Tomsia, A. P.; Ritchie, R. O. Bioinspired Structural Materials. *Nat. Mater.* **2015**, *14*, 23−36.
(2) Zhao, X.; Chen, X.; Yuk, H.; Lin, S.; Liu, X.; Parada, G. Soft Materials by Design: Unconventional Polymer Networks Give Extreme Properties. *Chem. Rev.* **2021**, *121*, 4309−4372.
(3) Wang, Y.; Naleway, S. E.; Wang, B. Biological and Bioinspired Materials: Structure Leading to Functional and Mechanical Performance. *Bioact. Mater.* **2020**, *5*, 745−757.
(4) Grubbs, R. B.; Grubbs, R. H. 50th Anniversary Perspective: Living Polymerization - Emphasizing the Molecule in Macromolecules. *Macromolecules* **2017**, *50*, 6979−6997.
(5) Leitgeb, A.; Wappel, J.; Slugovc, C. The ROMP Toolbox Upgraded. *Polymer* **2010**, *51*, 2927−2946.
(6) Yasir, M.; Liu, P.; Tennie, I. K.; Kilbinger, A. F. M. Catalytic Living Ring-Opening Metathesis Polymerization with Grubbs' Second- and Third-Generation Catalysts. *Nat. Chem.* **2019**, *11*, 488−494.
(7) Subnaik, S. I.; Hobbs, C. E. Flow-Facilitated Ring Opening Metathesis Polymerization (ROMP) and Post-Polymerization Modification Reactions. *Polym. Chem.* **2019**, *10*, 4524−4528.
(8) *Norbornene*. http://www.molbase.com/supplier/710794-product-1940070.html (accessed Feb 5, 2022).
(9) *cis-Cyclooctene*. http://www.molbase.com/supplier/795422-product-18698326-43205993.html (accessed Feb 5, 2022).
(10) *exo-5-Norbornenecarboxylic Acid*. https://www.sigmaaldrich.com/US/en/product/aldrich/718149 (accessed Feb 3, 2022).
(11) *Nadic Anhydride*. http://www.molbase.com/supplier/795422-product-17160981.html (accessed Feb 5, 2022).
(12) *5-Norbornene-2,3-Dicarboxylic Anhydride*. http://www.molbase.com/supplier/753902-product-3623928.html (accessed Feb 5, 2022).
(13) Chang, A. B.; Bates, C. M.; Lee, B.; Garland, C. M.; Jones, S. C.; Spencer, R. K. W.; Matsen, M. W.; Grubbs, R. H. Manipulating the ABCs of Self-Assembly via Low-$\chi$ Block Polymer Design. *Proc. Natl. Acad. Sci. U.S.A.* **2017**, *114*, 6462−6467.
(14) Bates, C. M.; Chang, A. B.; Momčilović, N.; Jones, S. C.; Grubbs, R. H. ABA Triblock Brush Polymers: Synthesis, Self-Assembly, Conductivity, and Rheological Properties. *Macromolecules* **2015**, *48*, 4967−4973.
(15) Chang, A. B.; Lin, T. P.; Thompson, N. B.; Luo, S. X.; Liberman-Martin, A. L.; Chen, H. Y.; Lee, B.; Grubbs, R. H. Design, Synthesis, and Self-Assembly of Polymers with Tailored Graft Distributions. *J. Am. Chem. Soc.* **2017**, *139*, 17683−17693.
(16) Zhang, K.; Yu, X.; Kuo, S. W. Outstanding Dielectric and Thermal Properties of Main Chain-Type Poly(Benzoxazine-: Co -Imide- Co -Siloxane)-Based Cross-Linked Networks. *Polym. Chem.* **2019**, *10*, 2387−2396.
(17) Otteny, F.; Studer, G.; Kolek, M.; Bieker, P.; Winter, M.; Esser, B. Phenothiazine-Functionalized Poly(Norbornene)s as High-Rate Cathode Materials for Organic Batteries. *ChemSusChem* **2020**, *13*, 2232−2238.
(18) Spring, A. M.; Qiu, F.; Hong, J.; Bannaron, A.; Yokoyama, S. Electro-Optic Properties of a Side Chain Poly(Norbornene-Dicarboximide) System with an Appended Phenyl Vinylene Thiophene Chromophore. *Polymer* **2017**, *119*, 13−27.
(19) Boyle, B. M.; Collins, J. L.; Mensch, T. E.; Ryan, M. D.; Newell, B. S.; Miyake, G. M. Impact of Backbone Composition on Homopolymer Dynamics and Brush Block Copolymer Self-Assembly. *Polym. Chem.* **2020**, *11*, 7147−7158.
(20) Biagini, S. C. G.; Gibson, V. C.; Giles, M. R.; Marshall, E. L.; North, M. Synthesis of Penicillin Derived Polymers Utilising Ring-Opening Metathesis Polymerisation Methodology. *Chem. Commun.* **1997**, *12*, 1097−1098.
(21) Sutthasupa, S.; Shiotsuki, M.; Sanda, F. Recent Advances in Ring-Opening Metathesis Polymerization, and Application to Synthesis of Functional Materials. *Polym. J.* **2010**, *42*, 905−915.
(22) Varlas, S.; Foster, J. C.; O'Reilly, R. K. Ring-Opening Metathesis Polymerization-Induced Self-Assembly (ROMPISA). *Chem. Commun.* **2019**, *55*, 9066−9071.
(23) Kong, P.; Drechsler, S.; Balog, S.; Schrettl, S.; Weder, C.; Kilbinger, A. F. M. Synthesis and Properties of Poly(Norbornene)s with Lateral Aramid Groups. *Polym. Chem.* **2019**, *10*, 2057−2063.
(24) Kammeyer, J. K.; Blum, A. P.; Adamiak, L.; Hahn, M. E.; Gianneschi, N. C. Polymerization of Protecting-Group-Free Peptides via ROMP. *Polym. Chem.* **2013**, *4*, 3929−3933.
(25) Golder, M. R.; Nguyen, H. V. T.; Oldenhuis, N. J.; Grundler, J.; Park, E. J.; Johnson, J. A. Brush-First and ROMP-Out with Functional (Macro)Monomers: Method Development, Structural Investigations, and Applications of an Expanded Brush-Arm Star Polymer Platform. *Macromolecules* **2018**, *51*, 9861−9870.
(26) Shibuya, Y.; Tatara, R.; Jiang, Y.; Shao-Horn, Y.; Johnson, J. A. Brush-First ROMP of Poly(Ethylene Oxide) Macromonomers of Varied Length: Impact of Polymer Architecture on Thermal Behavior and Li+ Conductivity. *J. Polym. Sci., Part A: Polym. Chem.* **2019**, *57*, 448−455.
(27) Wolf, W. J.; Lin, T. P.; Grubbs, R. H. Examining the Effects of Monomer and Catalyst Structure on the Mechanism of Ruthenium-Catalyzed Ring-Opening Metathesis Polymerization. *J. Am. Chem. Soc.* **2019**, *141*, 17796−17808.
(28) Slugovc, C.; Demel, S.; Riegler, S.; Hobisch, J.; Stelzer, F. The Resting State Makes the Difference: The Influence of the Anchor Group in the ROMP of Norbornene Derivatives. *Macromol. Rapid Commun.* **2004**, *25*, 475−480.
(29) Jiang, L.; Nykypanchuk, D.; Ribbe, A. E.; Rzayev, J. One-Shot Synthesis and Melt Self-Assembly of Bottlebrush Copolymers with a Gradient Compositional Profile. *ACS Macro Lett.* **2018**, *7*, 619−623.
(30) Nishihara, Y.; Inoue, Y.; Nakayama, Y.; Shiono, T.; Takagi, K. Comparative Reactivity of Exo- and Endo-Isomers in the Ru-Initiated Ring-Opening Metathesis Polymerization of Doubly Functionalized Norbornenes with Both Cyano and Ester Groups. *Macromolecules* **2006**, *39*, 7458−7460.
(31) Miyasako, N.; Matsuoka, S.; Suzuki, M. Ring-Opening Metathesis Polymerization of Endo- and Exo-Norbornene Lactones. *Macromol. Rapid Commun.* **2021**, *42*, No. 2170027.
(32) Yoon, K. H.; Kim, K. O.; Schaefer, M.; Yoon, D. Y. Synthesis and Characterization of Hydrogenated Poly(Norbornene Endo-Dicarboximide)s Prepared by Ring Opening Metathesis Polymerization. *Polymer* **2012**, *53*, 2290−2297.
(33) Kim, K. O.; Shin, S.; Kim, J.; Choi, T. Living Polymerization of Monomers Containing *endo*-Tricyclo[4.2.2.$0^{2,5}$]deca-3,9-diene Using


https://doi.org/10.1021/acs.macromol.2c01196
*Macromolecules* 2022, 55, 6671−6679

Second Generation Grubbs and Hoveyda−Grubbs Catalysts: Approach to Synthesis of Well- Defined Star Polymers. *Macromolecules* **2014**, *47*, 1351−1359.
(34) Yang, J. X.; Ren, L. X.; Li, Y. S. Ring-Opening Metathesis Polymerization of Cis-5-Norbornene-Endo-2,3-Dicarboxylic Anhydride Derivatives Using the Grubbs Third Generation Catalyst. *Chin. J. Polym. Sci.* **2017**, *35*, 36−45.
(35) Spring, A. M.; Yu, F.; Qiu, F.; Yamamoto, K.; Yokoyama, S. The Preparation of Well-Controlled Poly(N-Cyclohexyl-Exo-Norbornene-5, 6-Dicarboximide) Polymers. *Polym. J.* **2014**, *46*, 576−583.
(36) Cole, J. P.; Lessard, J. J.; Lyon, C. K.; Tuten, B. T.; Berda, E. B. Intra-Chain Radical Chemistry as a Route to Poly(Norbornene Imide) Single-Chain Nanoparticles: Structural Considerations and the Role of Adventitious Oxygen. *Polym. Chem.* **2015**, *6*, 5555−5559.
(37) Matson, J. B.; Grubbs, R. H. Synthesis of Fluorine-18 Functionalized Nanoparticles for Use as in Vivo Molecular Imaging Agents. *J. Am. Chem. Soc.*. **2008**, *130*, 6731−6733.
(38) Register, R. A.; Bishop, J. P.; et al. Poly(phenylnorbornene) from Ring-Opening Metathesis and its Hydrogenated Derivatives. *Macromol. Chem. Phys.* **2012**, *213*, 2027−2033.
(39) Hong, S. H.; Marczyk, A.; Trzaskowski, B.; et al. Decomposition of Ruthenium Olefin Metathesis Catalysts. *J. Am. Chem. Soc.* **2007**, *129*, 7961−7968.
(40) *Grubbs Catalyst M102*. https://www.sigmaaldrich.com/US/en/product/aldrich/579726 (accessed Feb 3, 2022).
(41) *Hoveyda-Grubbs Catalyst M720*. https://www.sigmaaldrich.com/US/en/product/aldrich/569755 (accessed Feb 3, 2022).
(42) Kingsbury, J. S.; Harrity, J. P. A.; Bonitatebus, P. J.; Hoveyda, A. H. A Recyclable Ru-Based Metathesis Catalyst. *J. Am. Chem. Soc.* **1999**, *121*, 791−799.
(43) Garber, S. B.; Kingsbury, J. S.; Gray, B. L.; Hoveyda, A. H. Efficient and Recyclable Monomeric and Dendritic Ru-Based Metathesis Catalysts. *J. Am. Chem. Soc.* **2000**, *122*, 8168−8179.
(44) Blencowe, A.; Qiao, G. G. Ring-Opening Metathesis Polymerization with the Second Generation Hoveyda-Grubbs Catalyst: An Efficient Approach toward High-Purity Functionalized Macrocyclic Oligo(Cyclooctene)S. *J. Am. Chem. Soc.* **2013**, *135*, 5717−5725.
(45) Song, K.; Kim, K.; Hong, D.; Kim, J.; Heo, C. E.; Kim, H. I.; Hong, S. H. Highly Active Ruthenium Metathesis Catalysts Enabling Ring-Opening Metathesis Polymerization of Cyclopentadiene at Low Temperatures. *Nat. Commun.* **2019**, *10*, No. 3860.
(46) Zhou, C.; Hou, C.; Cheng, J. Star Polymerization of Norbornene Derivatives Using a Tri-Functionalized Blechert's Olefin Metathesis Catalyst. *Polym. Chem.* **2020**, *11*, 1735−1741.
(47) Seo, J.; Lee, S. Y.; Bielawski, C. W. Dewar Lactone as a Modular Platform to a New Class of Substituted Poly(Acetylene)S. *Polym. Chem.* **2019**, *10*, 6401−6412.
(48) Yasir, M.; Liu, P.; Tennie, I. K.; Kilbinger, A. F. M. Catalytic Living Ring-Opening Metathesis Polymerization with Grubbs' Second- and Third-Generation. *Nat. Chem.* **2019**, *11*, 488−494.
(49) Liu, P.; Yasir, M.; Kilbinger, A. F. M. Catalytic Living Ring Opening Metathesis Polymerisation: The Importance of Ring Strain in Chain Transfer Agents. *Angew. Chem., Int. Ed.* **2019**, *58*, 15278−15282.
(50) Liu, P.; Dong, Z.; Kilbinger, A. F. M. Mono-Telechelic Polymers by Catalytic Living Ring-Opening Metathesis Polymerization with Second-Generation Hoveyda-Grubbs Catalyst. *Mater. Chem. Front.* **2020**, *4*, 2791−2796.
(51) Ogawa, K. A.; Goetz, A. E.; Boydston, A. J. Metal-Free Ring-Opening Metathesis Polymerization. *J. Am. Chem. Soc.* **2015**, *137*, 1400−1403.
(52) Lu, P.; Kensy, V. K.; Tritt, R. L.; Seidenkranz, D. T.; Boydston, A. J. Metal-Free Ring-Opening Metathesis Polymerization: From Concept to Creation. *Acc. Chem. Res.* **2020**, *53*, 2325−2335.
(53) Love, J. A.; Morgan, J. P.; Trnka, T. M.; Grubbs, R. H. A Practical and Highly Active Ruthenium-Based Catalyst That Effects the Cross Metathesis of Acrylonitrile. *Angew. Chem., Int. Ed.* **2002**, *41*, 4035−4037.
(54) Forcina, V.; García-Domínguez, A.; Lloyd-Jones, G. C. Kinetics of Initiation of the Third Generation Grubbs Metathesis Catalyst: Convergent Associative and Dissociative Pathways. *Faraday Discuss.* **2019**, *220*, 179−195.
(55) Piola, L.; Nahra, F.; Nolan, S. P. Olefin Metathesis in Air. *Beilstein J. Org. Chem.* **2015**, *11*, 2038−2056.
(56) Hoveyda, A. H.; Gillingham, D. G.; Van Veldhuizen, J. J.; Kataoka, O.; Garber, S. B.; Kingsbury, J. S.; Harrity, J. P. A. Ru Complexes Bearing Bidentate Carbenes: From Innocent Curiosity to Uniquely Effective Catalysts for Olefin Metathesis. *Org. Biomol. Chem.* **2004**, *2*, 8−23.
(57) Kumar, D. R.; Lidster, B. J.; Adams, R. W.; Turner, M. L. Mechanistic Investigation of the Ring Opening Metathesis Polymerisation of Alkoxy and Alkyl Substituted Paracyclophanedienes. *Polym. Chem.* **2017**, *8*, 3186−3194.
(58) Bielawski, C. W.; Grubbs, R. H. Increasing the Initiation Efficiency of Ruthenium-Based Ring-Opening Metathesis Initiators: Effect of Excess Phosphine. *Macromolecules* **2001**, *34*, 8838−8840.
(59) Mulhearn, W. D.; Register, R. A. Synthesis of Narrow-Distribution, High-Molecular-Weight ROMP Polycyclopentene via Suppression of Acyclic Metathesis Side Reactions. *ACS Macro Lett.* **2017**, *6*, 112−116.
(60) Jawiczuk, M.; Marczyk, A.; Trzaskowski, B. Decomposition of Ruthenium Olefin Metathesis Catalyst. *Catalysts* **2020**, *10*, No. 887.
(61) Michrowska, A.; Bujok, R.; Harutyunyan, S.; Sashuk, V.; Dolgonos, G.; Grela, K. Nitro-Substituted Hoveyda-Grubbs Ruthenium Carbenes: Enhancement of Catalyst Activity through Electronic Activation. *J. Am. Chem. Soc.* **2004**, *126*, 9318−9325.
(62) Kajetanowicz, A.; Grela, K. Nitro and Other Electron Withdrawing Group Activated Ruthenium Catalysts for Olefin Metathesis Reactions. *Angew. Chem., Int. Ed.* **2021**, *60*, 13738−13756.
(63) Bieniek, M.; Bujok, R.; Milewski, M.; Arlt, D.; Kajetanowicz, A.; Grela, K. Making the Family Portrait Complete: Synthesis of Electron Withdrawing Group Activated Hoveyda-Grubbs Catalysts Bearing Sulfone and Ketone Functionalities. *J. Organomet. Chem.* **2020**, *918*, No. 121276.
(64) Vinokurov, N.; Garabatos-Perera, J. R.; Zhao-Karger, Z.; Wiebcke, M.; Butenschön, H. A New, Highly Active Bimetallic Grubbs-Hoveyda-Blechert Precatalyst for Alkene Metathesis. *Organometallics* **2008**, *27*, 1878−1886.
(65) Luo, S. X.; Engle, K. M.; Dong, X.; Hejl, A.; Takase, M. K.; Henling, L. M.; Liu, P.; Houk, K. N.; Grubbs, R. H. An Initiation Kinetics Prediction Model Enables Rational Design of Ruthenium Olefin Metathesis Catalysts Bearing Modified Chelating Benzylidenes. *ACS Catal.* **2018**, *8*, 4600−4611.
(66) Grela, K.; Harutyunyan, S.; Michrowska, A. A Highly Efficient Ruthenium Catalyst for Metathesis Reactions. *Angew. Chem., Int. Ed.* **2002**, *41*, 4038−4040.
(67) Wakamatsu, H.; Blechert, S. A New Highly Efficient Ruthenium Metathesis Catalyst. *Angew. Chem., Int. Ed.* **2002**, *41*, 2403−2405.
(68) Engle, K. M.; Lu, G.; Luo, S. X.; Henling, L. M.; Takase, M. K.; Liu, P.; Houk, K. N.; Grubbs, R. H. Origins of Initiation Rate Differences in Ruthenium Olefin Metathesis Catalysts Containing Chelating Benzylidenes. *J. Am. Chem. Soc.* **2015**, *137*, 5782−5792.
(69) Nolan, S. P.; Piola, L.; Nahra, F. Olefin Metathesis in Air. *Beilstein J. Org. Chem.* **2015**, *11*, 2038−2056.
(70) Yoon, D. Y.; Yoon, K.; Kim, K. O.; Wang, C.; Park, I. Synthesis and Structure−property Comparisons of Hydrogenated Poly-(oxanorbornene-imide)s and Poly(norbornene-imide)s Prepared by Ring-Opening Metathesis Polymerization. *J. Polym. Sci., Part A: Polym. Chem.* **2012**, *50*, 3914−3921.


https://doi.org/10.1021/acs.macromol.2c01196
*Macromolecules* 2022, 55, 6671−6679